Gas Turbine Combined Cycle start-up and stress evaluation: a simplified dynamic approach

Iacopo Rossi, Alessandro Sorce, Alberto Traverso

Thermochemical Power Group, University of Genoa, Via Montallegro 1, Genoa, Italy

Corresponding author: Iacopo Rossi
e-mail: iacopo.rossi@edu.unige.it
Phone: +39 0103532463
Address: Via Montallegro 1, DIME sez. MASET, 16145 Genova (Italy)

ABSTRACT

The main topic of this work is the development and validation of a simplified approach for the dynamic analysis of a Gas Turbine Combined Cycle (GTCC), with a particular focus on start-up procedure and associated mechanical stresses on the steam turbine (ST). The currently deregulated energy market led GTCC to undergo frequent startups, a condition often not considered during plant design. Moreover, the time required for the start-up is crucial under an economical viewpoint, though it is constrained by mechanical stresses imposed to thick components by thermal gradients. The framework proposed in this work aims to improve the accessibility to simulation software by applying commonly used office suite – Microsoft Excel/Visual Basic – with acceptable reduction in accuracy. Simplicity of model allow fast computation and its exploitation can be pursued by non-qualified plant operators. The obtained tool can be than adopted to support decision process during plant operations. The developed tool has been validated for a hot start-up against field measurements supplied by Tirreno Power S.p.A. Italy. Data are recorded through control and monitoring sensors of a 390 MW multi-shaft combined cycle based on the GT AEN94.3 A4 frame, but the results can be easily generalized to other layouts. Simulation result and stress evaluations around the steam turbine (ST) rotor show good agreement with experimental data.

Keywords

HRSG Dynamic Model; Steam Turbine Stress Evaluation; GT Combined Cycle Start-up; Simplified Hybrid Modelling Approach; Experimental Validation

Highlights

- A simplified dynamic model of a GTCC bottoming cycle for plant start-up is presented
- Particular emphasis is placed on determining thermal stress on Steam Turbine rotor

- To enhance accessibility, the model is developed within Microsoft Excel environment
- The target system is the 390 MW Tirreno Power GTCC of Napoli Levante (Italy)
- Model validation is pursued against field measurement data (mean error of 5%)

NOMENCLATURE

Acronyms

BSE	Boiler Stress Evaluator
DTMS	Distributed Thermal Mass System
ECO	Economizer
EVA	Evaporator
FL	Full Load
FSNL	Full Speed No Load
GT	Gas Turbine
GTCC	Gas Turbine Combined Cycle
HP	High Pressure
HT	High temperature
HRSG	Heat Recovery Steam Generator
HX	Heat eXchanger
IGV	Inlet Guide Vane
IP	Intermediate Pressure
LCM	Lumped Capacitance Method
LP	Low Pressure
LT	Low Temperature
MEL	Minimum Environmental Load
R.H.	Relative Humidity
RH	Reheater
RSE	Rotor Stress Evaluation

SH	Super Heater
ST	Steam Turbine

Symbols

a	exponent of off-design relations
c_p	specific heat at constant pressure
E	Young module
f	model value
h	enthalpy
$\dot{m}$	mass flow rate
Nu	Nusselt number
$\dot{Q}$	heat power
T	temperature
T'	rate of change in temperature
Pr	Prandtl number
p	pressure
RE	Reynolds number
t	time
y	plant measurements
α	thermal coefficient
η	Heat Exchanger efficiency
ν	Poisson coefficient
ρ	density
σ	mechanical stress
τ	time constant

Subscripts

0	initial state

app	approach
att	attemperator
b	design condition (base load)
cool	cooled by the steam
exh	exhaust gas
gas	GT gas flow
inf	free stream condition
ss	design steady-state
stm	steam
unc	uncooled by the steam

1. INTRODUCTION

One of the main consequences of energy deregulations is the operational flexibility required to conventional power plants, which suddenly has become a key parameter. This has driven many changes to the whole energy field in recent years [1][2][3] . Energy plants started to undergo weekly and daily startups and shutdowns. As a consequence, plant components experience severe mechanical stress. In addition, the increasing share of renewable energy systems, together with restriction on pollutant emissions associated to energy production, have been deeply influencing the energy market [4][5][6][7][8]. Nowadays, the challenge deals with driving power plants from stand-still conditions to energy production as fast as possible. Hence, turbine manufacturers have focused their attention on engine quickness and their emissions, but the problem of efficient management of the whole plant persists.

In this regards, new ways to fasten the energy systems during startups [9] as well as in case of rapid transient load conditions [10], have been studied and tested [11][12][13][14][15]. Moreover, advanced monitoring technique were introduced to control the productive parameters of energy systems and life of their components [16][17][18][19][20]. Analysis on reliability and maintenance turned from a periodical approach to equivalent life-impact due to new high stressing working conditions. Modern technology and performance of present

GTCC plant [21] is also derived from studies based on energy system models, different in terms of software environment, purpose and structure [22][23][24][25][26][27].

In this scenario, the simulation software has gained significant importance in last decades and several approaches to model energy plants and their components have been studied and explored. Validation of software models consisted of testing the target systems under different situations and over several scenarios [28][29]. Despite of recent improvement in accessibility to the simulation tools, application of specific high-profile software [30][31] still require highly qualified users. From such considerations, Gulen *et al* .[32] proposed a different approach to model GTCC power plant in a simple way, in order to implement this kind of analysis through common Microsoft Office suite. Their idea was focused on creating a flexible and reliable tool to perform dynamic simulation with a particular emphasis on the Heat Recover Steam Generator (HRSG) and Steam Turbine (ST), the most stressed components [32]. The main goal of the approach unveils its novelty: in the field of dynamic analysis of energy system, to extend simulation software to a wider number of users This is pursued by proposing a framework that can be implemented through software usually available on normal desktop computer. The framework proposed here consists of a hybrid numerical and physical approach. This was critically analyzed in [33] by the Authors, and validation against experimental data has been presented for normal operating condition of the plant. Nevertheless, crucial operations of GTCC plant belong to start-up procedure. Integration of simplified method with rotor stress model proposed in [34] led to obtain a tool able to perform start-up analysis of a GTCC and predict stresses on ST.

2. REFERENCE SYSTEM

This work is based on the Tirreno Power 390MW GTCC of Napoli Levante (Italy). It is a three pressure levels HRSG, which produces steam for a steam turbine in a 1+1 multi-shaft layout. The gas turbine is a 270 MW Ansaldo AEN94.3A4. Global performance of the turbine is presented in Fig.1, where it is possible to see how the exhaust temperature increases during startups from full speed no load (FSNL) to the Minimum Environmental Load (MEL), which corresponds to 30 ppm CO emissions. MEL, for this GT frame, is reached around the 40% of GT base load, when the IGV are fully closed.

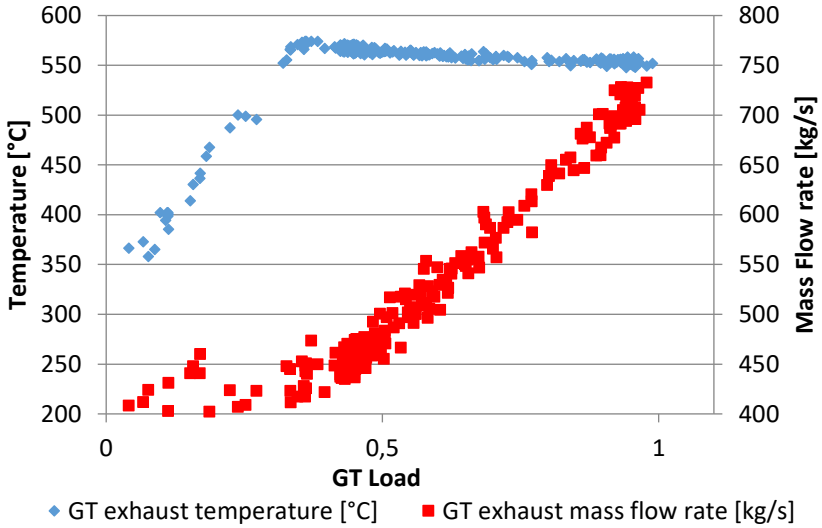

137

138 *Fig.1 GT exhaust temperature and mass flow rate*

139 The HRSG is arranged as shown in Fig.2. Reheater and superheater are split into two heat exchangers (HX).
140 These are connected through an attemperator (green square in figure) to cap the outlet steam temperature to
141 550°C, which is the maximum allowed temperature for the ST inlet.

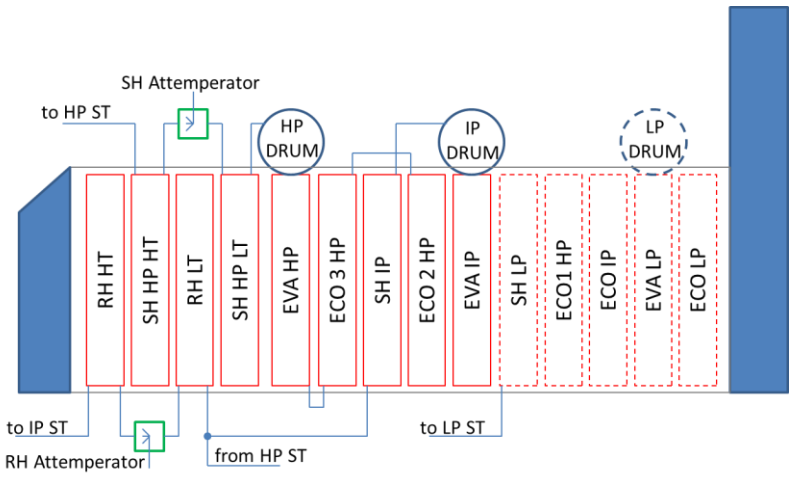

142

143 *Fig.2 HRSG heat exchangers arrangement for the three pressure levels drum-type HRSG with re-heating*

144 Evaporators are drum-type: the high pressure (HP) evaporator (EVA) is responsible for the 25% of the heat
145 recovery at base load, i.e. full speed full load (FSFL) at ISO condition. Presented model encloses HXs up to
146 the intermediate pressure (IP) EVA. It was considered not of interest to proceed further with modelling because
147 dynamic impact of load variation on last HXs is negligible. Moreover, with respect to the start-up phase, mainly
148 HP and IP mass flow rates are involved. However, extension of modeling process to the whole HRSG is
149 straightforward, thanks to repeatability of the approach. The provided methodology can be however applied

without any changes to 1+1 single shaft layout and, with minor changes, to a 2+1 layout, covering the whole GTCC state of art arrangement.

3. MODELING APPROACH

Since Gulen *et al.* have previously proposed the modelling approach [32] and its implementation has been already discussed and validated [33], so it is briefly described in the following section. It is important to remark that the model has to be defined in respect of the target GTCC plant taken into consideration. A series of main hypothesis were considered in order to reach a simplified representation of GTCC system [32]:

- Approach based on Lumped Capacitance Method (LCM)
- HRSG treated with Distributed Thermal Mass Theory (DTMS)
- HRSG heat exchangers (HX) geometry simplified as described by Dechamps in [35]
- Temperature of metal coincides with steam temperature

In view of the system analyzed, two more specific hypotheses were introduced. As shown in Fig.3:

- Steam generation rate is directly proportional to the exhaust flow rate.
- Drum pressure and steam flow are directly linked.

These hypothesis, well confirmed by data, have been already validated against experimental measurements in [33] and they led to an absolute average error lower than 10°C for all the HXs, 2 kg/s for steam flow rate and 4 bar for the pressure drums. In Fig.3b control system performs an additional pressurization for values of steam flow rate higher than 85% to create a “pressure reserve”, that is useful to regulate the steam turbine to fast control the grid frequency. A specific function, designed on experimental data, was defined to capture this behavior. This highlights that the model should integrate the influence of the control logics on the plant. Moreover, to make the model capable of well representing the plant behavior, strong importance is given to the numerical training process. This is based on real field data measurements and consists of a calibration of the numerical parameters involved in the model computation. The training is refined by considering R2 results of the statistical analysis, in order to obtain a good fitting of the experimental data [33]. It should be remarked that influence of ambient conditions on the recovery process is strong, thus the model should not be used outside the ambient temperature range used during the training process.

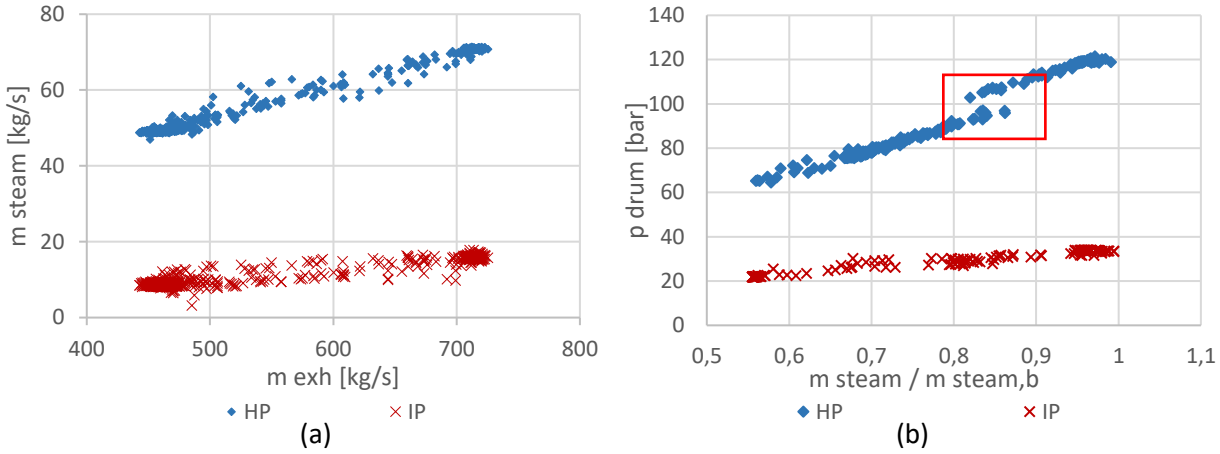

176

177 *Fig.3 Field measurements HRSG normal operating condition: (a) HP and IP steam mass flow rate as function of exhaust mass flow rate and (b) HP*

178 *and IP drum pressure as a function of steam flow rate. A square highlights the pressurization reserve operation on the drum pressure*

179 **3.1 Training process**

180 The training process, which was based on 10 days of working data (Fig.3 is based on the same data set), is
181 necessary to obtain a good description of the system In this case, the adopted data are focused on the ambient
182 conditions close to ISO (as summarized in Table 1). It follows a matrix where it is possible to see the
183 distribution of the parameters that define the general conditions of the training (Fig 4).It can be noticed that all
184 those external condition are not correlated between them, with the exception of the inlet ambient temperature
185 and Relative Humidity. All the operating range and ambient conditions are well covered by the training data.
186 Data shows how production is mainly concentrated close to MEL. During the 10 days period the power plant
187 experienced two shutdown and consequent start-up.

188

	GT Load	**Ambient condition**		
	[MW]	T [°C]	p [mbar]	R.H. [%]
MAX	264	21	1017	100
AVERAGE	137	13	1012	66
MIN	112	8	1004	37
STD	54.7	2.6	3.6	22.8

189 *Table 1 Training power and ambient condition*

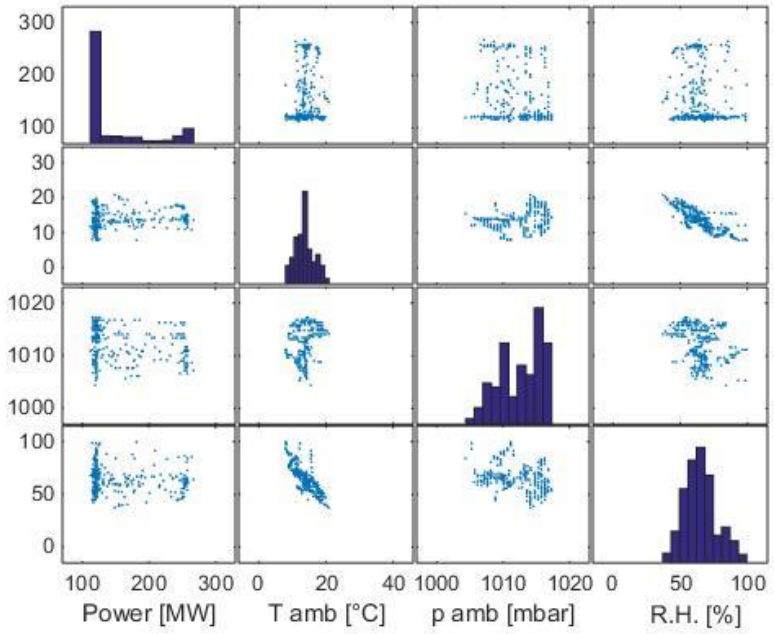

Fig.4 Distribution of experimental data adopted for the training of the model

Validity of the involved parameters was demonstrated around ±10°C from mean ambient temperature used for the training. Out of this range a new set of numerical equations - obtained from a new training process - should be used to avoid non acceptable steady state errors. Main parameters involved in the training of the HRSG model are the scale factors *k* and the ΔT_{app} [33], which describe the HRSG off-design behavior. The scale factors *k* are used to evaluate temperature of the hot gas as they enter the particular HX. The second one represents the difference in approach temperature between gas and water side at the end of the recovery process of the investigated HX. Some other minor parameters are involved in the training process, such as pressure function or fitting exponent *a*. More information and considerations, together with the model validation for normal operating conditions, can be found in [33]. This research is mainly focused on start-up simulation.

3.2 Start-up procedure

Start-up plays a key role among other operating conditions of a power plant. This operation is composed by a sequence of pre-defined steps that have to be repeated recursively each time the plant is started up. This implies that start-up procedure deserves a modeling profile of its own. During start-up, main important

parameters to be controlled deal with security of operations and structural constraints of the bottoming cycle. Great importance is given to the allowable stress by the steam turbine (ST) rotor, which, in some power plants, is monitored by the Rotor Stress Evaluator (RSE). Another important monitoring system is the Boiler Stress Evaluator (BSE), which acts on the pressure ramp during the start-up, in order to limit drum stress cycle.

An analysis of the impact of control logics on the start-up phase is presented. The initial conditions depend on the shutdown interval of the plant. This influences the average temperature of all sensitive components of the plant and the residual pressure in the drum, with a deep influence on the ramping procedure in terms of constraints and times. Table 2 encloses the three usually adopted cluster for initial conditions: Cold, Warm and Hot. Start-up time is estimated in table 2 for plant with power ranges between 80 MW and 400 MW [36]. Please note that in this case the expected time represents the time for the whole procedure, i.e. from GT ignition to HP and IP bypass closed. A cold start-up can include additional operations such as generation of auxiliary steam and vacuum creation. The start-up time differences are related to the bottoming cycle requirements (HRSG and ST) while Gas Turbine start-up is basically independent of its standstill time.

Start-up condition	**Standstill**	**Expected time for start-up**
	[h]	[min]
COLD	120	120-170
WARM	48	80-120
HOT	8	40-60

Table 2 Summarization of start-up conditions

Normative laws (NFPA 85 or API616) [37][38] impose to purge the HRSG by speeding up the GT. This procedure has a small influence on the general condition of the plant, i.e. the cooling effect on the HRSG is negligible, but it requires 7 to 13 minutes. Purge credit can be used to reduce the start-up time [1][39]. In general, three different logics that govern the ramping up of the plant within start-up procedure can be defined [32]. These should be adapted and modeled for each target plant, in view of the installed equipment (presence of a final desuperheater or attemperation). Pollutant emission is another constraint to consider. GT behavior may inhibit some load due to high pollutant gases produced. Even though the MEL law prescribes no emission limit, the GT avoids the working points with high NO_x emissions, in particular.

To replicate start-up procedure, some more equations in addition to the original set [33] must be considered. Firstly, drum pressure starts to rise when the incoming energy is sufficiently high. The energy balance around EVA is obtained through boiler temperature and the boiling conditions persisting in the evaporator (Eq.1). Forcing term is again associated to exhaust mass flow and its temperature as it reaches the drum (which is computed considering factor *k*, as it has been previously described).

$$Q_{eva}(t) = \eta \cdot \dot{m}_{exh} \cdot c_p(k_{EVA}T_{exh} - T_{EVA}) \cdot \tau \quad (1)$$

Once the necessary conditions to increase the drum pressure are reached, the heat exchanged with the evaporator drives the pressure gradient (Eq.1) and it is bounded by the BSE (Table 3). The admissible drum pressure is defined according to the UNI EN 12952 limit. During real start-up, drum vent valves and bypass valves controls the admissible pressure gradient: while the vented mass flow rate is considered negligible, the most relevant pressure effect was modeled. This parameter is monitored within the model simulation and the computed gradients are recursively limited, if necessary.

Drum pressure	[bar]	0	10	20	40	50	100
Maximum positive gradient	[bar/min]	0.2	1.24	2.05	3.44	4	7

Table 3 Example of pressure gradient of BSE control system

Thermal inertias have been evaluated both for IP drum and HP drum and they are summarized in Table 4. These values have been derived from mass considerations on metal, water and steam. On this basis, inertia should be changed instantaneously with simulation, in consideration of water level in the drum. Instead, constant values have been used by considering mean properties of water and steam in between 5 and 60 bar. Steam to water ratio volume in the drums was persisting at the start-up of the plant (which is a fixed value imposed by control routines).

To evaluate Eq.1, considering *i* the present time step, *i-1* evaporator temperature value is used for pressure computation and the boiling point is computed through a specific function [40]. This function is based onIAPWS Industrial Formulation. The *i-th* temperature is then linked to the energy coming to the evaporator and to its pressure rising gradient. This computation is done continuously as long as the normal operating conditions of plant are reached, i.e. the pressure corresponding to minimum load that persists in the HP and IP drums.

		IP		HP	
	Thermal capacitance [kJ/kgK]	**Total Mass** [kg]	**Thermal inertia** [MJ/K]	**Total Mass** [kg]	**Thermal inertia** [MJ/K]
Steam	1.9	16	0.03	164	0.3
Water	4.186	16240	68	41813	175
Metal	0.466	3980	2	22159	10
Total		**20236**	**70**	**64136**	**185**

Table 4 IP and HP drums characteristic data

Once the GTCC reaches the minimum load, the simulation tool switches to computation system presented in [33]. In terms of drum pressure values, minimum operating conditions corresponds to 63 bar for HP drum and 21 bar for IP drum, against a nominal value at design point of 124 bar and 34 bar, respectively. Mass flow is computed consequently. During the start-up, steam flow is not directly correlated to the exhaust mass flow rate yet. In particular, at the very beginning of the procedure, a series of events take place simultaneously, which are difficult to represent. Steam flow generation is hardly quantifiable, due to bypass opening/closing and vent systems used to assist drums pressurization. Globally, incoming energy must be compared to the energy necessary for boiling process plus the effect of pressurization of the drum. As long as the energy that arrives in the evaporator does not suffice to boil water in the drum, no steam can be generated. Then, once the steam generation starts, the effect of pressurization intervenes on the generated steam, together with other system events. While the model, due to its simplified nature, does not consider the venting effect, the pressurization of the drums is represented by the variation in internal energy in Eq.2. Internal energy can be expressed as a function of enthalpy and pressure. The volume is given by the physical dimensions of drums and the imposed drum levels are considered for the start-up. This time variation of energy within the drum is linked to internal energy, which is associated to condition experimented by the working fluid.

$$\begin{gathered} {}^{dQ}/_{dt} = {}^{dU}/_{dt} \\ Q = \dot{m}_{stm} r\tau + Q_{eva} \\ U = \rho V u \end{gathered} \tag{2}$$

As long as the ramping up of the system is taking place, Eq.2 is used. Once the steam generation begins, the flow generated is diverted from the ST through a by-pass cascade system. Diverted steam flow is driven to the

condenser, as long as the requisites for admission in ST are not reached. Admission conditions of the ST depend on starting temperature of the rotor and this impacts the speed-up gradient imposed to the turbine. However, the driving steam flow used to speed up the turbine is a portion of the whole amount generated and in general it consists of 5% of the nominal value [34]. This suffices to drive the ST to the Full Speed No Load (FSNL) condition. After that, blow-off and bypass are closed and the whole steam generated in the process is now admitted to the ST.

In this phase, bypass valves are governed by pressure persisting behind them. Consequently, the bypass may be closed after some minutes the ST has reached the FSNL condition. This happens when the GT loads the drum too much during the speed ramp of the ST. In this case, the bypass is used to rate down the drum pressure to its pre-defined value. This is evident looking at Fig.5, where the bypass is fully closed after the load ramp of ST is concluded and all the generated steam is admitted in the ST. Once the start-up procedure is completed, the simulation system turns to the normal operating condition. This is managed continuously within model computations, since the main model hypothesis are same both for start-up and normal operating conditions. In terms of computational procedures, main differences in between start-up and normal operative conditions are determined in the resolution of forcing term. As stated in [32], input data are divided in intervals in which a linear hypothesis for input changes can be made. This apply also to start up data, but since during start-up, change of the input are faster, an higher resolution is mandatory to obtain a reliable signal. Therefore, start-up simulation requires the higher resolution in order to capture the whole ramp.

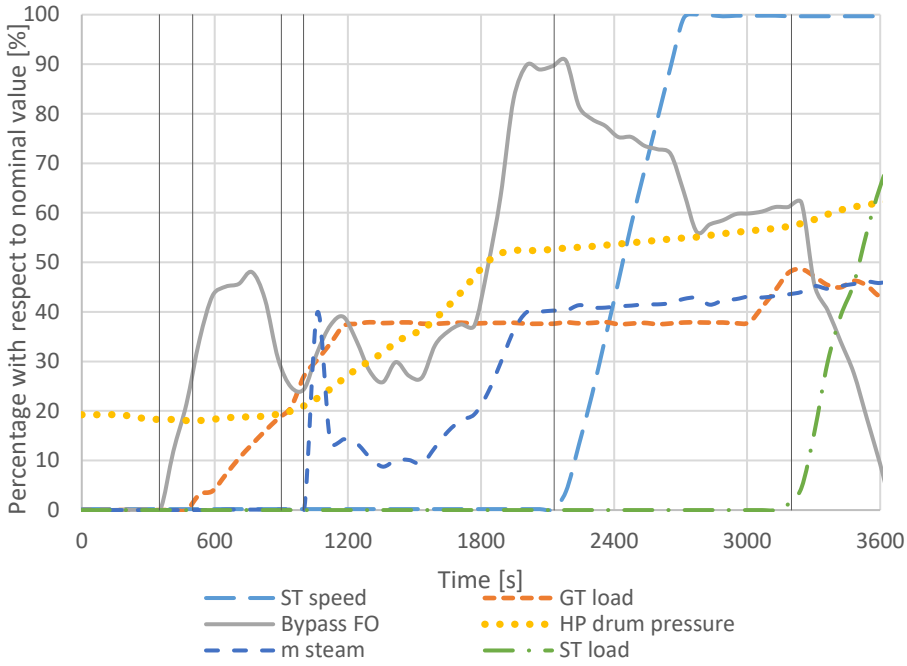

Time [s]	Event
400	Bypass opening
500	GT loading
900	Hp pressure arises
1000	Steam gen. begins
2200	ST acceleration
3200	ST loading
3600+	Bypass closed

Fig.5 Measured Data: Bypass valve fractional opening with respect to ST load with event table. In figure vertical black indicators show sequentially the events reported in table on the right.

4. MEASUREMENT SYSTEM

Intensive properties as pressure and temperature, are well measured along all the HRSG steam side, enabling the calculation of the temperature increase and pressure losses in quite any HX. On the other side, the extensive properties (i.e. the mass flow rates) measurement require more complex pipe arrangements and are measured in fewer positions. Steam mass flow rate measurement system is arranged as shown in Fig.6, where measurement points are highlighted with blue vertical marks. Since they are placed just before the bypass system, difference in mass flow rate generated in between model and experimental data can be evaluated also during the start-up. This is essential, since bypass valves are opened during the ramping of the system and they drive the flow to the condenser. Unfortunately, impact of Drum Vent Valves is hardly quantifiable. Schematic detail neglects some components and does not discriminate between high and low temperature SH and RH and associated attemperation system presented in figure 2. On the other hand, the bypass path is highlighted, together with its valve and attemperating system. Attemperation is generated by extracting a small fraction of water from pumping system: evaporation process of water releases high amount of heat without involving high mass flow. This is done for both HP and IP compounds. In general, the measurement system is the typical industrial instrumentation, with lower precision than in the commissioning phase, but high robustness, typical

accuracy is (+/- 2.5 K for temperature probes, +/- 1% F.S. for pressure probes, +/- 1.5÷5 % of FS for steam mass flow rate measurement [41]).

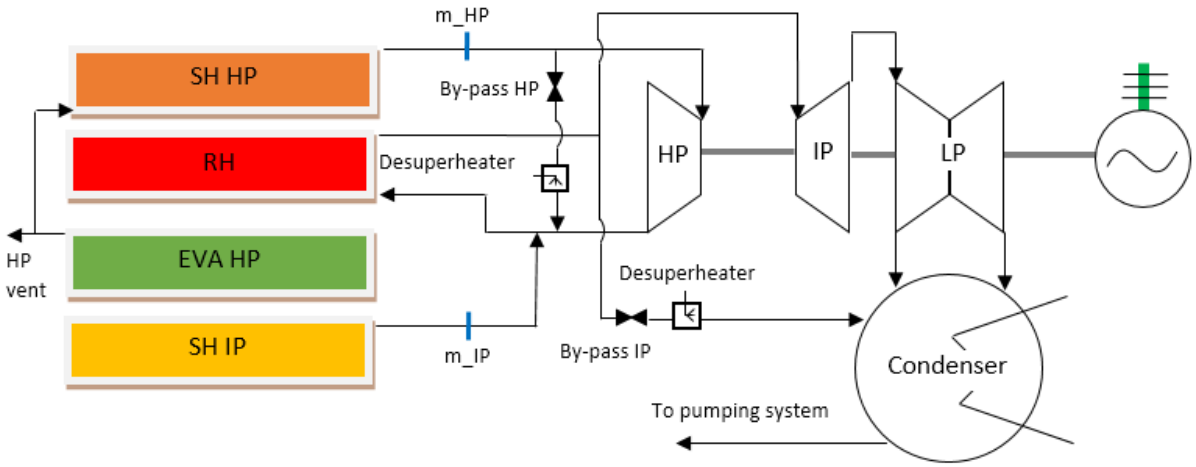

Fig.6 Schematics of cascade bypass and steam mass flow rate measurement point

5. ROTOR STRESS ANALYSIS

Within start-up procedure, The thermoelastic stress of the rotor represents a key factor as one of the main physical constraints imposed to the system. The issue is about bounding thermal gradient on the steam turbine rotor within some defined values, which depend on start-up condition. The aim is to limit fatigue stresses on ST rotor. Rotor Stress Evaluator (RSE) control monitors the load margin, that is, a parameter based on the rotor temperature. In case the load margin reaches a certain threshold, the RSE control system intervenes by reducing GT load ramp and slowing the start-up operation. In term of economic objectives, the optimization involves increasing the operational speed without exceeding the load margin limit. Therefore, it is of strong importance to monitor the rotor temperature, in order to understand the allowable gradient for the ST rotor. Industrial state of the art suggests that, in addition to the steam temperature, the ST stator case internal surface temperature is measured and this value is assumed equal to the external surface temperature of the rotor itself. On this basis, the temperature of the center of the rotor is evaluated through a model for heat conduction inside the rotor. To create a flexible model, the relation between steam temperature and surface metal temperature were taken into account. In terms of dynamic response, the forcing term is the mass of steam investing the rotor and its temperature. External surface temperature is the first one to respond to the forcing term, while the inner temperature follows the ramp with a certain delay. This generates a difference in temperature throughout

the rotor and the consequential stress. Initial conditions determine how the rotor is stressed. Calculation of RSE and its meaning is well-analyzed in [34]. In [42] a procedure was outlined to compute the working life consumption globally due to this kind of stress. However, some information linked to the topic is mentioned hereby. In the present model, RSE evaluations are started by considering the heat coefficient as given by a fraction of steam flow (Eq.3). This proposes the variation of enthalpy proportional to variation in steam flow.

$$h(t) = h_b \left(\frac{\dot{m}_{stm}(t)}{\dot{m}_{stm,b}} \right)^a \quad (3)$$

Exponential coefficient ranges between 0.8 and 1. Other well-known, non-dimensional groups are involved in this process: Table 5 summarizes their regime values [42].

Coefficent	Regime values	Unit
h	2172	W/m2K
Nu	22218	-
Re	9.5*10^7	-
Pr	1.147	-

Table 5 Heat exchange properties of steel of the rotor surface

Biot number, as well as Fourier number is then computed for evolving process. The radius is discretized at four different values. External and internal temperatures of rotor are finally computed using zero-orders Bessel function, as suggested in [34]. Stresses are finally computed by considering Eq.4, which considers the difference between average temperature and external source temperature. Mechanical properties of the rotor metal Cr-Mo-V steel are summarized in Table 6, which refers to [43]. Inputs to this part of the model are steam temperature and steam mass flow, computed by HRSG model presented previously.

$$\sigma_T = \frac{E \cdot \alpha}{1-\nu} (\bar{T} - T_{ext}) \quad (4)$$

Coefficent	Regime values	Unit
Young Module	205000	MPa
Thermal coefficent	0.000012	1/K
Poisson coefficent	0.3	-

Table 6 Mechanical properties of Cr-Mo-V steel

6. RESULTS

The HRSG model has been previously validated [33] within the normal operating range of the plant (i.e. over the MEL). This work validates the developed model for start-up simulation. Influence of the ambient condition in this case is marginal, since the higher amount of weather-conditioned parameters are used only once the start-up is substantially accomplished. Under this viewpoint, load factor *k* and difference in temperature approach are the main involved parameters. Furthermore, start-up routine is the same for every ambient situation. Input values for start-up simulation (GT load and exhaust temperature) are shown in Fig.7, together with exhaust mass flow. This figure is enriched with two vertical lines that indicate two different steps in the procedure: synchronization and MEL condition. These are identically reported in the successive graphs of this section in order to give an idea of the continuity of these events and how they are linked to bottoming cycle response. Actually, in the early steps, temperature used for simulation is not the one measured at gas turbine outlet, but the one entering the HRSG. These values coincide at regime, but they may differ in early phase, since GT blow-off are opened until synchronization with the grid is reached (first indicator in Fig.7) and this effect is measured at the inlet of the HRSG rather than at GT outlet. This mitigates the temperature variation between the 5^{th} and 10^{th} minute (Fig.7). Blow-off generate a consistent difference between the two considered temperatures (for a maximum difference close to 45°C), which are however identical during the GT ramp, after blow-off are closed. Indeed right after blow-off are closed, GT is ramped up and reaches MEL condition (last indicator). Simulation results are presented starting from first HXs down to the IP line.

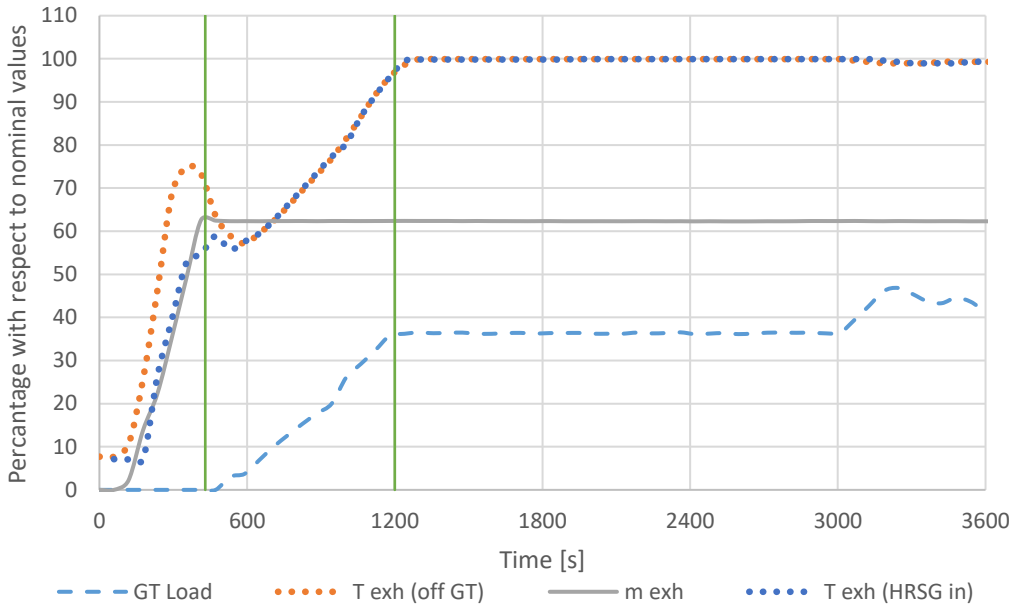

377

378 *Fig.7 Start-up data of GT load, exhaust mass flow and exhaust temperature at GT outlet and HRSG inlet. Vertical green indicators shows*

379 *respectively synchronization and GT minimum load*

380 First HX compounds to be presented are the RHs and the SHs (Fig.8). RH is the real first HX to meet the

381 forcing heat flux (Fig.8a). This is reflected by temperature profile, which is strictly linked to forcing term:

382 exhaust flow temperature. In general, this is true for all the first HXs [33]. A consistent dead time (three to

383 four steps) is included to capture the early phase dynamics of the start-up; otherwise, assumptions on which

384 the model is based would lead to a global faster response in this stage.

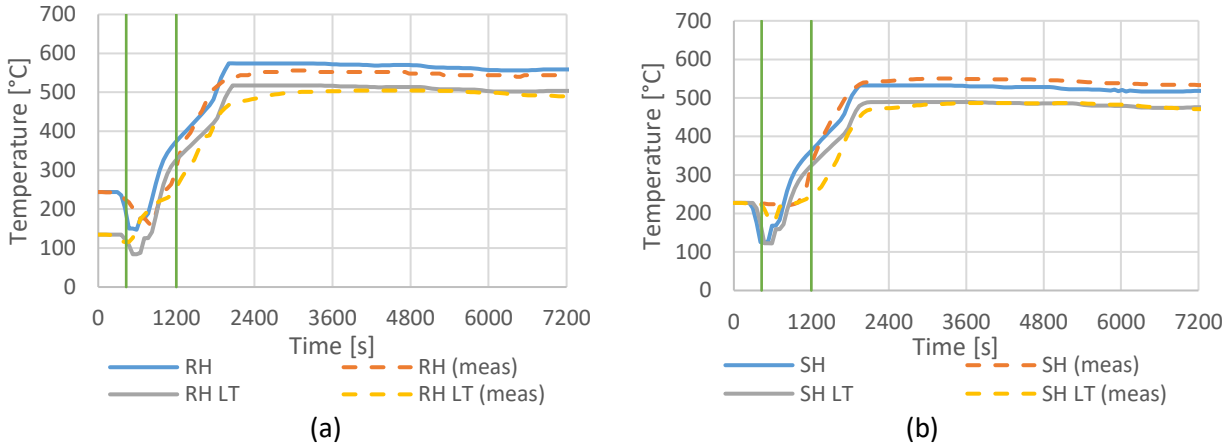

385

386 *Fig.8 RH and SH HP temperature profiles from simulation results*

387 Within these initial results, SH response is of great importance for rotor stress analysis, since it represents

388 the temperature profile of the steam entering the ST (Fig.8b). In terms of dynamic response, the anticipation

389 of model response is mitigated by dead time imposed, while the ramping gradient is globally correct. The

faster response of the model with respect to the measured values of temperature in the first 1000 seconds is related to the negligible steam mass flow entering the HXs, which causes a delay in the measured values – this because the fluid is the means which transfers temperature information. In fact, the model computes a rising in temperature of HX metal compound also before steam starts to be generated in the EVA.

On the other hand, experimental data are obtained through the installed measurement system. The temperature probes that acquire the measurement of steam temperature are located outside the HRSG. Therefore, they require a steam mass flow rate to register the increase of the pipes temperature within HRSG. GT takes about 1200 seconds (20 minutes) to reach a load level (around 36.5%) which ensure an exhaust temperature at HRSG reach their nominal condition. In this regard, the higher difference in results is reached between 10 and 15 minutes after start-up of the plant (Figure 8). Globally, the higher average error in absolute term is related to RH response, which is close to 16°C during the start-up simulation. The mean absolute error associated to the SH is lower: it is about 11°C. These values have a strong importance because they are part of the inputs for stress evaluation of the rotor.

Evaporators play an important role in the start-up procedure: in particular, the HP EVA drives the pressure rising evolved throughout the HP line and consequently generates the steam. Results regarding HP EVA, together with HP ECO, are illustrated below: temperature (Fig.9), drum pressure and generated steam flow (Fig.10). In Fig.10b it is also possible to observe the influence of internal energy balance of drum pressure in respect of generated steam. The dotted line is the result of computation without considering Eq.2 and it shows the high influence of HP pressurization on steam generation.

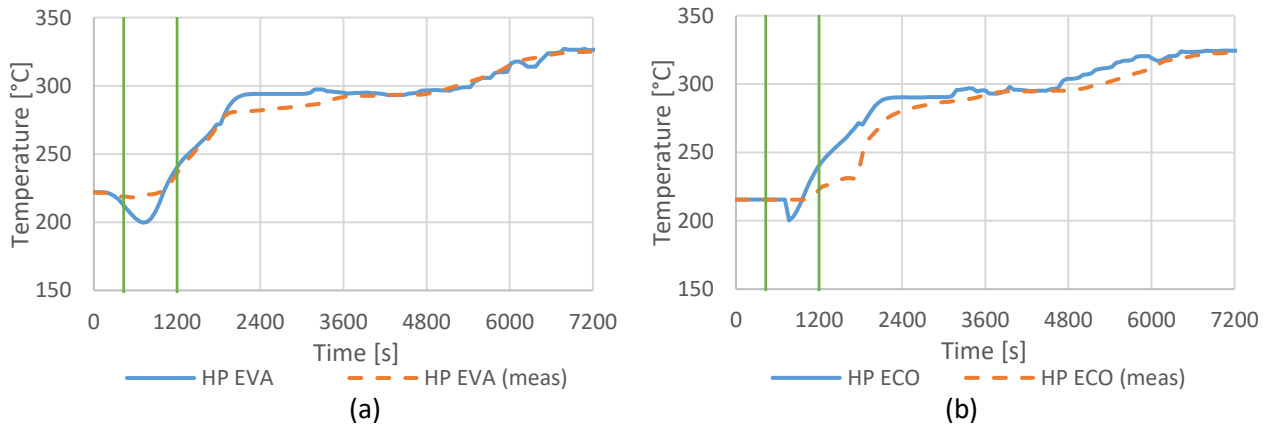

Fig.9 HP EVA and HP ECO model temperature profiles

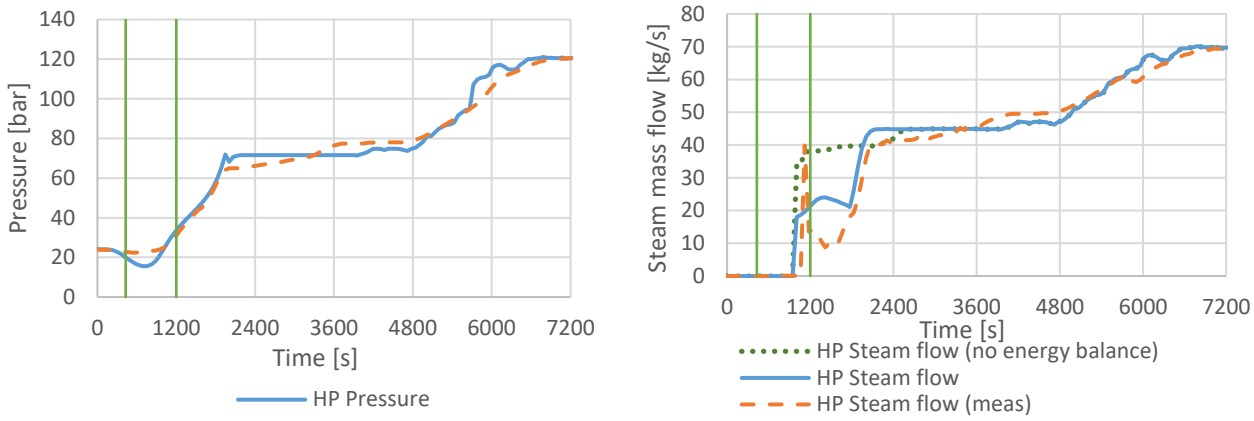

411

412 *Fig.10 HP EVA pressure and steam generation simulation results*

413 Response of HP ECO (Fig.9b) is a bit higher with respect to measured data; still the rising gradient is
414 correct. Evaporator resulting profile is well tracked by the model (Fig.9a), except initial simulations when a
415 consistent reduction in temperature is present. This part is governed by thermal inertia proposed previously,
416 which fits well with the increasing pressure instead. Moreover, the model generates a good response in terms
417 of rising time and gradient (Fig.10a).

418 On the other hand (Fig.10b), steam generation starts when the evaporator pressure rises (after 1800
419 seconds). In the first part of steam generation a series of effects occur simultaneously and most of them cannot
420 be reproduced by this simplified model layout, as stated previously. Nevertheless, the model describes the
421 pressurization effect of the drum, which reduces the produced steam. It is important to remark that computing
422 the correct steam flow produced during the start-up, together with SH and RH temperature profile, is of strong
423 importance for the RSE evaluations, since the steam flow drives the turbine acceleration. The mean average
424 error for the steam mass flow generation (considering absolute values) is about 3 kg/s during the start-up. The
425 remaining difference between model simulations and experimental measurements is mainly caused by the
426 venting system. This is the same in case of IP line. Therefore, it follows the description of the IP section,
427 starting from the SH compound down to the IP EVA (Fig.11).

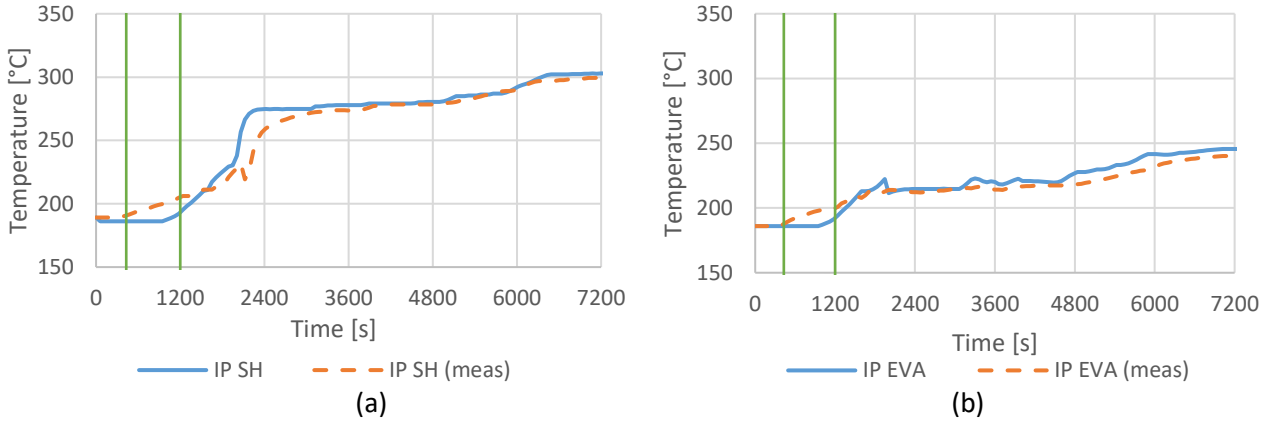

Fig.11 SH IP and EVA IP simulation results

Looking at the SH IP (Fig.11a), it is possible to observe nearly the same behavior as in the case of HP section, again a bit higher with respect to measured temperature. For the IP EVA (Fig.11b), the response of the system is slower in the first instants, while the rising gradient is higher (20th to 25th minutes), after that, a smooth trend is presented. Results from IP drum pressure (Fig.12a) and steam mass flow generated (Fig.12b), are explained below.

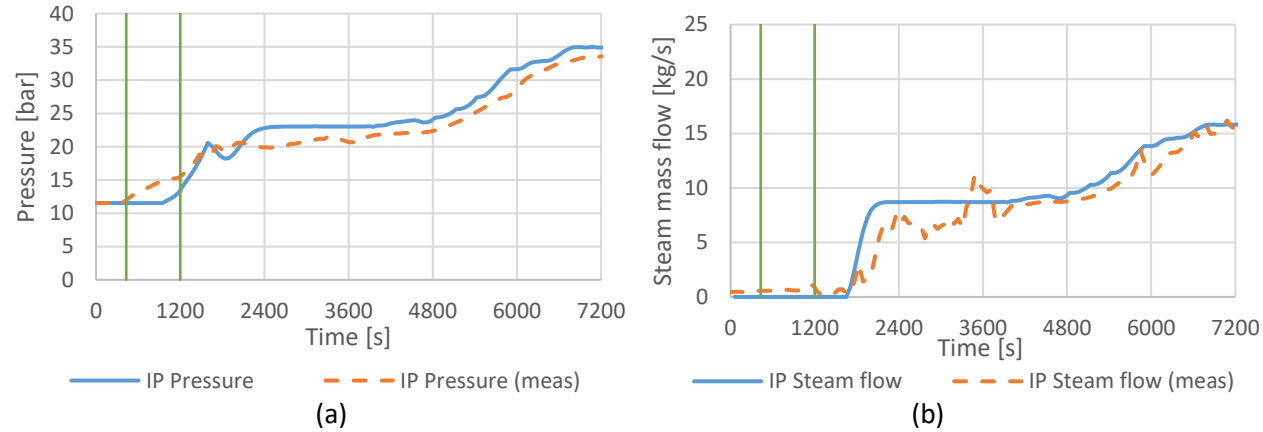

Fig.12 Pressure and steam mass flow computed by the model for the IP section

The problem of model response for IP pressure drum profile is the same as observed for the IP EVA temperature, plus a significant discontinuity when the model turns from starting condition to normal operating ones when IP drum reaches 21 bar. While the starting time of flow generation, is well captured by the model. Again, the differences in the very first part can be accounted to the vent actions. IP steam mass flow represents another input for RSE model. In this case the average error is about 1 kg/s in absolute terms. As long as simulation is running, it is possible to compute RSE analysis with steam temperature. The stress evaluation

involves both the IP and the HP part of the rotor. Which is a welded-disk type. Their characteristics data are summarized in Table 6.

	Rotor diameter [mm]	**Shroud diameter** [mm]
HP	725	800
IP	810	1022

Table 6 Geometrical data of rotors

In Fig.13, evolution of estimated stresses is presented both for HP and IP rotors. Since the simulated scenario presents hot start-up conditions, steam flow initially cools the ST shaft and external temperature of the rotor drops to steam values. This influences the distribution of the rotor stresses: on the external surface the shaft undergoes traction stress and vice versa for the inner surface. Model results are compared with experimental data computed by RSE model of [34]. It is possible to notice a consistent agreement in between simulation computations and what is given by using experimental data. The main differences lay on the IP rotor stresses, where rising gradient is more significant than what is computed from experimental data, as summarized in Table 7. Both of them present higher stress value i.e. conservative results and this is also valid for differences in rising gradient (in particular for IP section, as stated previously).

	HP	**IP**
Model peak value [MPa]	126	135
	-225	-241
Experiment-based peak value [MPa]	120	129
	-223	-231
Error (ABS) [MPa]	6	6
	2	10

Table 7 Simulation results for computed stresses

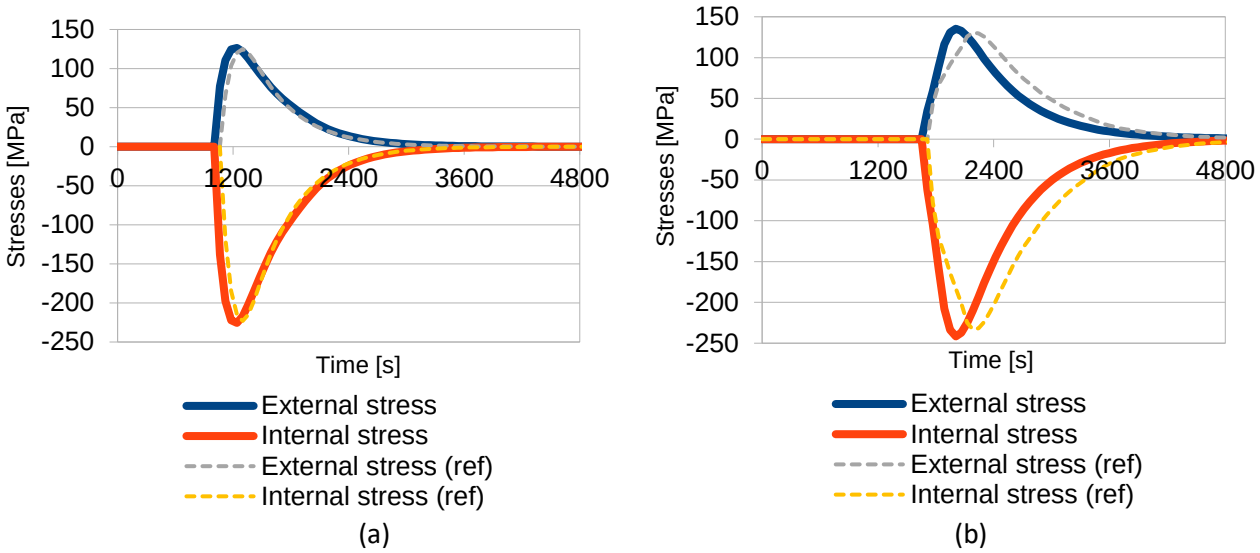

457

458 *Fig.13 Stresses computed by the RSE model within simulation, both for HP and IP rotor*

459 ## 7. CONCLUSIONS

460 The work proposes a simulation tool based only on Excel/Visual Basic for GTCC plants, which synthetizes
461 results from more complex software analysis. The model is able to perform fast simulations of normal
462 operating conditions as well as start-up conditions. The time required to compute a start-up case like the one
463 presented in this paper is lower than 1 minute on a desktop system.

464 In addition to normal operating condition equations [33], which were triggered and tested against
465 experimental data, additional equations were used to take into account typical aspects of the start-up phase. In
466 particular, the effect of HRSG pressurization over steam production rate and the technological constraints due
467 to allowable thermal cyclic stresses for thick components (e.g. HP Drum and Steam Turbine) are considered.
468 Those general equations were evaluated taking into account the geometry of the actual system and validated
469 against measurements. In particular, the model considers stresses on the HP and IP steam turbine rotor during
470 transient, as those are the parameters that the run up system controls during GTCC load ramp. Simplicity of
471 interface makes the tool suitable for fast simulations and easily exploitable by end-users, with a particular
472 consideration of supporting decisions of operators in real plants. In this way they can have quickly available a
473 projection of plant operations. The general approach has already been discussed and validated in [33]. Here,
474 the presented start-up case study proposes to compute Rotor Stress Evaluator (RSE) analysis on ST rotor. The
475 objective of the model is to provide reliable information about ST stress, which derive from plant start-up
476 procedure. This has been done by considering the approach discussed by several author [34][41].

The model provides reliable results for dynamic simulation of load transients, with a good consistency of all the thermodynamic parameters of the generated steam. Even if average deviations are higher than in normal operating condition (worst case, RH temperature presents a mean error almost 4 time higher during start-up rather than normal operating condition [33]), the goal of the model is however reached. RSE computation on turbine rotors shows a mean error of 6 MPa in absolute terms (less than 5%), with respect to maximum peaks of reference stresses [34]. Start-up simulation results are globally reliable, with some deviations in the early phases of the operations for some neglected effects as the drum vent valves that do not compromise the general goal of the model.

The aforementioned model is able to return results, which are crucial for start-up optimization were the effect of a certain stress in terms of ST damage must be compared against the reduction of the start-up time, often necessary to gain chance of production in the electricity market. Further elements of investigation will focus on the coupling with advanced FEM simulation tool for RSE and the automation of training phase of HRSG parameters.

REFERENCES

[1] Husak, M., Jones., Tegel, D., 2006, "Combined Cycle Plant Operational Flexibility", POWER-GEN International 2006, November 28-30, 2006, Orlando, FL.

[2] Balling L., 2011, "Alstom's HRSG – Optimized for Today's Flexibility Requirements", POWER-GEN International, 13-15 December, 2011, Las Vegas, NV, USA.

[3] Henkel N., Schmid E., Gobrecht E., 2008, "Operational Flexibility Enhancements of Combined Cycle Power Plants", POWER-GEN Asia 2008, Kuala Lumpur, Malaysia.

[4] Brouwer A. S., van den Broek M., Seebregts A., Faaij A., 2015, "Operational flexibility and economics of power plants in future low-carbon power systems", Applied Energy, vol. 156, 107-128.

[5] Rao A.D., Francuz D.J., 2013, "An evaluation of advanced combined cycles", Applied Energy, vol. 102, pp 1178-1186.

[6] Pan M., Aziz F., Li B., Perry S., Zhang N., Bulatov I., Smith R., 2016, “Application of optimal design methodologies in retrofitting natural gas combined cycle power plants with CO2 capture”, Applied Energy, vol. 161, pp 695-706.

[7] Majoumerd M. M., De S., Assadi M., Breuhaus P., 2012, “An EU initiative for future generation of IGCC power plants using hydrogen-rich syngas: Simulation results for the baseline configuration”, Applied Energy, vol. 99, pp 280-290.

[8] Alqahtani B.J., Patino-Echeverri D., 2016, “Integrated solar combined cycle power plants: paving the way for thermal solar”, Applied Energy, vol. 169, pp 927-936.

[9] Tica A., Guéguen H., Dumur D., Faille D., Davelaar F., 2011, “Start-Up of Combined Cycle Power Plants”, IFAC World Congress 2011, Milan, Italy.

[10] Benato A., Stoppato A., Mirandola A., 2015, “Dynamic behaviour analysis of a three pressure level heat recovery steam generator during transient operation”, Energy, vol.90, pp 1595-1605.

[11] Alobaid, F., Postler, R., Strhole, J., Epple, B., Hyun-Gee, K., 2008, “Modeling and investigation start-up procedures of a combined cycle power plant”, Applied Energy 85, pp. 1173-1189.

[12] Casella, F., Pretolani, F., 2006, “Fast Start-Up of A Combined Cycle Power Plant: A Simulation Study with Modelica,” 5th International Modelica Conference, September 4-6, 2006, Vienna, Austria.

[13] Balling L., 2011, “Fast cycling and rapid start-up: new generation of plants achieves impressive results”, Modern Power System, Erlangen, Germany.

[14] Casella F., Farina M., Righetti., Scattolini R., Faille D., Davelaar F., Tica A., Gueguen H., Dumur D., 2011, “An optimization procedure of the start-up of Combined Cycle Power Plants”, IFAC World Congress, Milan, Italy.

[15] Mertens N., Alobaid F., Starkloff R., Epple B., Kim H.G., 2015, “Comparative investigation of drum-type and once-through heat recovery steam generator during start-up”, Applied Eergy, vol. 144, 250-260.

[16] Sorce A., Martini A., Traverso A., Torelli G., 2014, “Heat steam recovery generator health assessment basing on reconciled measurements”, ASME Turbo Expo 2014, Dusseldorf, Germany.

527 [17] Martini A., Sorce A., Traverso A., 2014, “Field measurement reconciliation for combined cycle heat
528 recovery steam generator monitoring”, ASME Turbo Expo 2014, Dusseldorf, Germany.

529 [18] Cafaro S., Veer T., 2009, "Diagnostics of Combined Cycle Power Plants: Real Applications to
530 Condition Based Maintenance”, 9th International Conference on Heat Engines and Environmental Protection.

531 [19] Narasimhan S., and C. Jordache, 2000, “Data Reconciliation and Gross Error Detection: an intelligent
532 use of process data”, Gulf Publishing Company, Houston, Texas.

533 [20] Syed M. S., Dooley K.M., Madron F., Carl Knopf F., 2016, “Enhanced turbine monitoring using
534 emissions measurements and data reconciliation” Applied Energy, vol. 173, pp 355-365

535 [21] Kotowicz J., Job M., Brzęczek M., 2015, “The characteristics of ultramodern combined cycle power
536 plants” Energy, vol. 92, pp 197-211.

537 [22] Benato A., Bracco S., Stoppato A., Mirandola A., 2016, “Dynamic simulation of combined power plant
538 cycling in the electricity market”, Energy Conversion and Management, vol. 107, pp 76-85.

539 [23] Tica A., Guéguen H., Dumur D., Faille D., Davelaar F., 2012, “Design of a combined cycle power
540 plant model for optimization”, Applied Energy, vol. 98, pp 256-265.

541 [24] Bakhshmand S. K., Saray R. K., Bahlouli K., Eftekhari H., Ebrahimi A., 2015, “Exergoeconomic
542 analysis and optimization of a triple-pressure combined cycle plant using evolutionary algorithm”, Energy,
543 vol. 93, 555-567.

544 [25] Alobaid F., Strohle J., Epple B., Kim H.G., 2009, “Dynamic simulation of a supercritical once-through
545 heat recovery steam generator during load changes and start-up procedures”, Applied Energy, pp 1274-1282.

546 [26] Sindareh-Esfahani P., Ghaffari A., Ahmadi P., 2014, “Thermodynamic modeling based optimization
547 for thermal systems in heat recovery steam generator during cold start-up operation”, Applied Thermal
548 Engineering, vol. 69, pp 286-296.

549 [27] Alobaid F., Karner K., Belz J., Epple B., Kim H.G., 2014, “Numerical and experimental study of a heat
550 recovery steam generator during start-up procedure”, vol. 64, pp 1057-1060.

551 [28] Gulen, S.C., Smith, R.W., 2010, “Second law efficiency of the Rankine Bottoming Cycle of a
552 Combined Cycle Power Plant”, J.Eng. Gas Turbines & Power, Vol. 132.

553 [29] Cha, H., Song, Y.S., et al., 2011, “Dynamic simulations of a HRSG system for a given startup/shutdown
554 curve”, ASME Paper IMECE2011-62468, ASME 2011 Int. Mech. Eng. Congress & Expo., November 11-17,
555 2011, Denver, CO, USA.

556 [30] Casella F., Pretolani F., 2006, “Fast Start-up of a Combined-Cycle Power Plant: a Simulation Study
557 with Modelica”, 5th International Modelica Conference 2006, Vienna, Austria.

558 [31] El Hfni B., Bouskela D., Lebreton G., 2011, “Dynamic modelling of a combined cycle power plant
559 with ThermoSysPro”, 8th International Modelica Conference 2011, Dresden, Germany.

560 [32] Gulen, S.C., Kim, K., 2013, “Gas Turbine Combined Cycle dynamic simulation: a physics based simple
561 approach”, Journal of Engineering of Gas Turbines and Power, vol. 136.

562 [33] Rossi I., Sorce A., Traverso A., Pascucci F., 2015, “A simplified hybrid approach to dynamic model a
563 real HRSG”, ASME Turbo Expo 2015, Montreal, Canada.

564 [34] Mitrovic D., Zivkovic D., 2010, “Computation of working life consumption of a steam turbine rotor”,
565 Journal of the pressure vessel technology, vol. 132.

566 [35] Dechamps, P.J., 1995 “Modelling the transient behaviour of heat recovery steam generator”, Proc.
567 Instn. Mech. Engrs. 1995, Vol. 209, pp 265-273.

568 [36] Kelhofer, R. et al., 2009, “Combined-Cycle Gas & Steam Turbine Power Plants”, McGraw-Hill.

569 [37] National Fire Protection Association NFPA 85: Boiler and Combustion Systems Hazards Code, 2015
570 Edition

571 [38] American Petroleum Institute, API 616 Gas Turbines (Gas Turbine for the Petroleum, Chemical, and
572 Gas Industry Service) 5th edition 2011

573

574 [39] Gulen S. C., Jones C. M., 2011, “GE’s next generation CCGT plants: operational flexibility is the key”,
575 Modern Power Systems, pp 16-18

576 [40] http://www.cheresources.com/staff.shtml, last access 29/10/2015

577 [41] VDI 2048 Part I, Uncertainties of measurement during acceptance tests on energy-conversion and
578 power plants- Fundamentals, October 2000, VDI - Gesellschaft Energietechnik.

579 [42] Grosso M., Sansoni F., Sorce A., Monti M., Pascucci F., Razzoli R., 2016, “Influence of Start-up
580 Management on the Residual Life of a Large Steam Turbine Shaft”, Proceeding at ISROMAC 2016

581 [43] Einfluß moderner Verfahren der Stahlerschmelzung auf das Zeitstandverhalten dickwandiger Bauteile
582 aus 1 %-CrMoV-Stählen, Kommission der Europäischen Gemeinschaften ISBN 92-826-2504-4 (1991)

583